Mon. Not. R. Astron. Soc. **335,** 233–240 (2002)

Integrated spectral evolution of Galactic open clusters

Andrés E. Piatti,[1⋆] Eduardo Bica,[2⋆] Juan J. Clariá,[3⋆] João F. C. Santos, Jr[4⋆] and Andrea V. Ahumada[3⋆]

[1]*Instituto de Astronomía y Fisica del Espacio, CC 67, Suc. 28, 1428, Capital Federal, Argentina*
[2]*Universidade Federal do Rio Grande do Sul, Departmento de Astronomía, CP 15051, Porto Alegre, 91500-970, Brazil*
[3]*Observatorio Astronómico, Laprida 854, 5000 Córdoba, Argentina*
[4]*Departamento de Física, ICEx, UFMG, CP 702, 30123-970 Belo Horizonte, MG, Brazil*

Accepted 2002 April 26. Received 2002 March 25

ABSTRACT

We present a library of 47 open-cluster integrated spectra, mostly obtained at CASLEO (San Juan, Argentina) in the range $3600 < \lambda < 7400$ Å, which are made available at CDS. The data are combined with previous spectra to obtain 10 high signal-to-noise ratio basic templates in the young and intermediate-age domains, which are also provided in the library. These Galactic disc templates represent the increased time resolution spectral evolution of a stellar population unit around the Solar metallicity level. The improved signal-to-noise ratio of the present templates with respect to previous template lists, together with their increased time resolution, allowed us to improve the fundamental parameters of some open clusters. The present spectral library will be useful for several astrophysical applications, particularly for population syntheses of star-forming giant galaxies.

Key words: techniques: spectroscopic – open clusters and associations: general – galaxies: individual: Milky Way – galaxies: star clusters.

1 INTRODUCTION

Star clusters can be viewed as stellar population units of a given age and metallicity (Bica & Alloin 1986a,b). Star cluster integrated spectra, their templates and grids of spectral properties have been used for population synthesis and interpretation of galaxy spectra (e.g. Bica 1988). The templates are averages of similar cluster spectra utilized with the purpose of improving the spectrum signal-to-noise (S/N) ratio. They are useful for comparisons and derivation of individual cluster parameters in the Milky Way (e.g. Santos & Bica 1993; Piatti, Clariá & Bica 1999; Ahumada et al. 2000) and in external galaxies, e.g. M31 and NGC 5128 (Jablonka, Alloin & Bica 1992; Jablonka et al. 1996, 1998). Recently, a large library of cluster and galaxy spectra has become available at CDS (Santos et al. 2001), which includes the open clusters observed at ESO (Table 1). Nevertheless, it is important to further develop cluster libraries, especially in certain metallicity ranges, also improving the time resolution. In the star cluster observations of Bica & Alloin (1986a), young and intermediate-age clusters were mostly sampled in the Large Magellanic Cloud (LMC), while only a few Milky Way disc clusters were included. In recent years an effort was made at Complejo Astronómico El Leoncito (CASLEO, San Juan, Argentina) to observe relatively high surface brightness star clusters in the Magellanic Clouds and in the Galaxy, especially unstudied or poorly studied open clusters (e.g. Piatti, Bica & Clariá 1998a; Ahumada et al. 2001). In general terms, Galactic open clusters are characterized by large angular sizes and low star concentrations. Nevertheless, many of them appear to be concentrated objects suitable for integrated spectroscopic observations.

In the present study we gather these individual Galactic open-cluster integrated spectra and average them into templates, together with previously available spectra, with a view to obtaining the highest possible S/N ratio and higher time resolution to study their integrated light evolution. In the next section, a list of the integrated spectra of open clusters used in the present paper is given, together with a description of the observation of an additional cluster. The objects showing similar spectral properties are grouped into templates in Section 3. A discussion of the new templates as well as a revision of the fundamental parameters for some individual clusters is presented in Section 4. The final conclusions of this work are provided in Section 5.

2 THE DATA

2.1 Spectra selection

The individual spectra used to construct the template spectra come from different works on open clusters suitable for integrated spectroscopic observations (column 3 of Table 1). In these

⋆E-mail: andres@iafe.uba.ar (AEP); bica@if.ufrgs.br (EB); andrea@mail.oac.uncor.edu (JC); claria@mail.oac.uncor.edu (JC); jsantos@fisica.ufmg.br (JFCS); andrea@mail.oac.uncor.edu (AVA)

Table 1. Fundamental parameters of the cluster sample.

Name	Spectrum	Ref.	$E(B-V)$	Ref.	Age (Myr)	Ref.
NGC 2158	ESO	44	0.55 ± 0.10	37	3000 ± 1000	37
vdB-RN 80	CASLEO	28	0.38 ± 0.04	28	4.5 ± 1.5	28
NGC 2368	CASLEO	28	0.12 ± 0.03	28	50 ± 10	28
Berkeley 75	CASLEO	28	0.05 ± 0.02	28	3000 ± 1000	28
Haffner 7	CASLEO	28	0.10 ± 0.05	28	100 ± 10	28
ESO 429-SC 13	CASLEO	28	0.00 ± 0.03	28	100 ± 50	28
NGC 2635	CASLEO	28	0.25 ± 0.05	23,28,45	1000^{+500}_{-200}	23,28,45
NGC 2660	ESO	44	0.39 ± 0.02	38,39	1100 ± 100	38,39
UKS 2	CASLEO	8	0.30 ± 0.10	3,8	800 ± 200	3,8
Ruprecht 83	CASLEO	45	0.45 ± 0.05	43,45	55 ± 20	45
Hogg 3	CASLEO	28	0.15 ± 0.02	28	75 ± 25	28
BH 87	CASLEO	28	0.10 ± 0.02	28	150 ± 50	28
Westerlund 2	CASLEO	1	1.67 ± 0.15	1	2.5 ± 0.5	1
NGC 3293	LNA	13	0.25 ± 0.04	34,35,36	6 ± 1	22,35,36
Bochum 12	CASLEO	28	0.25 ± 0.05	21,28	45 ± 15	28
Pismis 17	CASLEO	28	0.51 ± 0.07	21	4.5 ± 1.5	28
Hogg 11	CASLEO	28	0.32 ± 0.05	21	8 ± 5	28
ESO 93-SC 8	CASLEO	8	0.50 ± 0.15	7,8	4000 ± 1000	7,8
NGC 3603	ESO	13	1.46 ± 0.02	13,14,15,16	2 ± 1	13,14,15,16
Melotte 105	CASLEO,ESO	9,13	0.42 ± 0.03	9,10,13	300 ± 50	9,10,13
BH 132	CASLEO	9	0.60 ± 0.05	9	150 ± 50	9
Hogg 15	CASLEO	9	1.10 ± 0.05	9,20	20 ± 10	9,20
NGC 4755	LNA	13	0.39 ± 0.05	13,17,18,19	8 ± 2	13,17,18,19
Pismis 18	CASLEO	2	0.50 ± 0.05	2	1200 ± 400	2
NGC 5606	CASLEO	28	0.50 ± 0.05	5,28,29	6 ± 2	28,29
NGC 5999	ESO	13	0.45 ± 0.05	4,13	300 ± 100	4,13
NGC 6031	CASLEO	4	0.15 ± 0.15	4	200 ± 100	4
Ruprecht 115	CASLEO	4	0.60 ± 0.05	4	500 ± 100	4
Pismis 22	CASLEO	11	2.00 ± 0.10	11	40 ± 15	11
Ruprecht 119	CASLEO	12	0.80 ± 0.05	12	15 ± 10	12
Ruprecht 120	CASLEO	4	0.65 ± 0.10	4	100 ± 100	4
NGC 6178	CASLEO	11	0.20 ± 0.05	11	40 ± 10	11
Lyngå 11	CASLEO	9	0.12 ± 0.03	9	450 ± 50	9
Westerlund 1	CASLEO	1	4.30 ± 0.20	1	8 ± 3	1
NGC 6216	CASLEO	11	0.45 ± 0.05	11	35 ± 15	11
NGC 6231	LNA	13	0.45 ± 0.05	13,25,26	4 ± 1	13,25,26
NGC 6253	CASLEO	2	0.25 ± 0.05	2,6	4000 ± 1000	2,6
BH 217	CASLEO	9	1.40 ± 0.10	9,45	20 ± 15	9,45
NGC 6318	CASLEO	12	1.20 ± 0.05	12	20 ± 20	12
BH 245	CASLEO	12	2.25 ± 0.05	12	15 ± 10	12
Ruprecht 130	CASLEO	11	1.20 ± 0.05	11	50 ± 10	11
NGC 6520	ESO	13	0.43 ± 0.02	13,19	190 ± 40	13,19
NGC 6603	ESO	13	0.50 ± 0.02	13,24,27	350 ± 100	13,24,27
NGC 6611	LNA	13	0.85 ± 0.05	13,30,31,32	3 ± 2	13,30,31,32
Ruprecht 144	CASLEO	9	0.32 ± 0.02	9	150 ± 50	9
NGC 6705	ESO	44	0.42 ± 0.03	40,41	250 ± 50	40,42
NGC 6756	ESO	13	0.70 ± 0.10	13,33	300 ± 100	13,33

References: (1) Piatti et al. (1998a), (2) Piatti et al. (1998b), (3) Bica, Ortolani & Barbuy (2000), (4) Piatti et al. (1999), (5) Moffat & Vogt (1973), (6) Bragaglia et al. (1997), (7) Bica, Ortolani & Barbuy (1999), (8) Bica et al. (1998), (9) Ahumada et al. (2000), (10) Piatti & Clariá (2001), (11) Piatti et al. (2000b), (12) Piatti et al. (2000a), (13) Santos & Bica (1993), (14) Hofmann, Seggewiss & Weigelt (1995), (15) Pandey, Ogura & Sekiguchi (2000), (16) Melnick, Tapia & Terlevich (1989), (17) Sanner et al. (2001), (18) Sagar & Cannon (1995), (19) Kjeldsen & Frandsen (1991), (20) Piatti et al. (2002), (21) Moffat & Vogt (1975), (22) Herbst & Miller (1982), (23) Moitinho (2001b), (24) Sagar & Griffiths (1998), (25) Baume, Vázquez & Feinstein (1999), (26) Sung, Bessell & Lee (1998), (27) Bica, Ortolani & Barbuy (1993), (28) Ahumada et al. (2001), (29) Vázquez et al. (1994), (30) Belikov et al. (2000), (31) Belikov et al. (1999), (32) Hillenbrand et al. (1993), (33) Delgado, Alfaro & Cabrera-Caño (1997), (34) Balona (1994), (35) Feinstein & Marraco (1980), (36) Turner et al. (1980), (37) Christian, Heasley & Janes (1985), (38) Sandrelli et al. (1999), (39) Hartwick & Hesser (1973), (40) Sung et al. (1999), (41) Johnson, Sandage & Wahlquist (1956), (42) Brocato, Castellani & Digiorgio (1993), (43) Topakas & Fenkart (1982), (44) Bica & Alloin (1986a), (45) this work.

studies the cluster fundamental parameters were determined from the Balmer line equivalent widths and from the comparison of the observed spectra with the template spectra defined by Bica & Alloin (1986a,b), Bica (1988) and those in Santos et al. (1995). In the young and intermediate-age ranges the former templates include LMC and some Galactic open clusters with moderate time resolution, while the latter templates deal separately with clusters in both Magellanic Clouds, and the time resolution is high for young LMC templates. The cluster spectra cover slightly different visible wavelength ranges and some of them also extend

towards near-infrared (near-IR) wavelengths. The limitations of the spectra in the bluest wavelengths resulted from a combination of several factors, among which are cluster surface brightness, detector response and amount of reddening. Table 1 lists the cluster names, the sites of observation and the cluster integrated spectrum references along with the adopted reddening estimates and ages. For some clusters, reddening and age values derived from integrated spectrum analyses are the only ones available. For some others, we complemented the integrated spectroscopic information with results coming from photometric studies. Whenever possible, we estimated weighted averages from the different values of reddening and age. We also averaged both spectra of Melotte 105 obtained by Santos & Bica (1993) and Ahumada et al. (2000). In some few cases, we redetermined the cluster fundamental properties by comparing the cluster spectra with the present more complete spectral sample of clusters with known fundamental parameters (see Section 4.1). References of the sources of the cluster integrated spectra as well as of some other detailed studies on the respective clusters are listed in columns 3, 5 and 7 of Table 1. Finally, we decided not to include the integrated spectra of Hogg 12 (Ahumada et al. 2001), Pismis 19 (Piatti et al. 1998b) and NGC 6067 (Santos & Bica 1993). Hogg 12 was considered by Moffat & Vogt (1975) as a probable random fluctuation of the field star density. Pismis 19 appears to be the only object in the sample, for which the integrated spectrum reflects the evolutionary stage of a cluster with an age between 500 Myr and 1 Gyr, but has a low S/N ratio. We did not include the spectrum of NGC 6067 in the sample, since it was obtained with an early detector at a lower resolution.

2.2 Observations and reductions of additional data

We also included in the cluster sample the integrated spectrum of Ruprecht 83, also known as BH 80 (van den Bergh & Hagen 1975), which we obtained with the 2.15-m telescope at CASLEO during a run in 1995 May. We employed a REOSC spectrograph with a Tektronics charge-coupled device (CCD) with 1024 × 1024 pixels and a grating of 300 line mm^{-1} in two different configurations. On the one hand, we obtained spectra from 3500 to 7000 Å with an averaged dispersion and resolution of 140 Å mm^{-1} (3.46 Å pixel^{-1}) and 14 Å, respectively. Dispersion and resolution values were taken from the wavelength coverage and FWHM of the He–Ar comparison lamp spectra. On the other hand, we obtained spectra from 5800 to 9200 Å with a similar dispersion (3.36 Å pixel^{-1}) and a resolution of 17 Å. We employed an OG 550 filter with the aim of eliminating the second-order contamination for $\lambda > 5800$ Å. In both setups the slit width and the total field along the slit were 4.2 arcsec and 4.7 arcmin, respectively, with the latter allowing us to sample the cluster background regions. The slit was oriented in the east–west direction and the observations were made by scanning the slit across Ruprecht 83 in the north–south direction in order to obtain a proper sampling of the cluster. We took eight exposures of 15 min each summing an hour in the blue and red wavelength ranges, respectively. We observed spectrophotometric standards to calibrate the observed spectra. Stars LTT 4364, EG 274 and LTT 7379 (Stone & Baldwin 1983) were used in the blue range, whereas in the red range we added to these standard stars the hot dwarf star HD 160 233 (Gutiérrez-Moreno et al. 1988) to eliminate telluric absorption bands. For instrumental calibration purposes, nightly we took frames of He–Ar comparison lamps between and after the object observations, as well as bias and dome, twilight sky and tungsten lamp flat-fields. The integrated spectra were reduced at the Astronomical Observatory of Córdoba (Argentina) using the IRAF[1] facilities. Several other sets of integrated spectra were also obtained during the same run, and they are partially presented in Piatti, Clariá & Bica (2000b), where a detailed description of the reduction procedures, the errors and the method employed to derive the age and reddening values is given. Basically, the method consists in measuring the equivalent widths of the Balmer lines and comparing the cluster spectrum with cluster spectra of known parameters. Thus, we derive $E(B-V) = 0.40 \pm 0.15$ and an age of 55 ± 20 Myr for Ruprecht 83. Fig. 1 shows the observed integrated spectrum of this cluster, the same spectrum corrected for the derived foreground-reddening value and the present template Ye (Section 4) that best matches the corrected spectrum. The derived $E(B-V)$ colour excess shows very good agreement with the previous estimate of Topakas & Fenkart (1982), based on RGU photographic photometry of 93 stars observed in the field of the cluster. As far as we know, no age value has been estimated for Ruprecht 83.

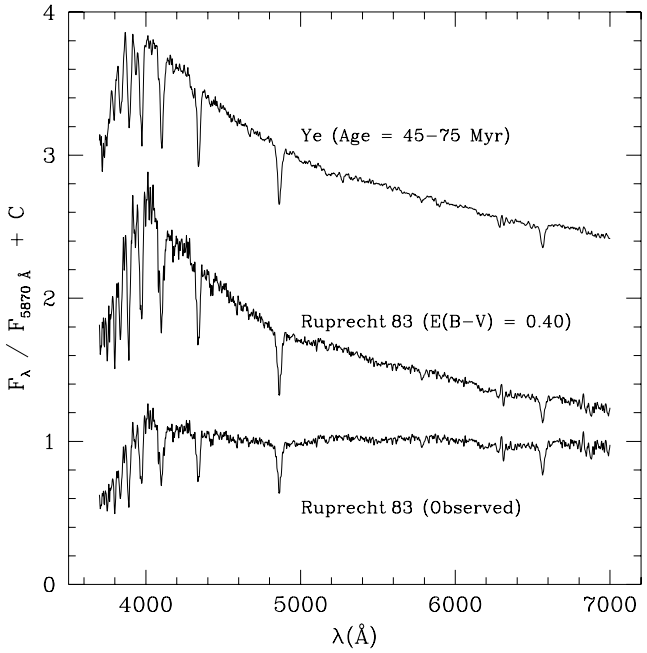

Figure 1. Observed integrated spectrum of Ruprecht 83, the same spectrum corrected for the derived foreground-reddening value and the present template Ye, which best matches the corrected spectrum. The spectra are normalized at $\lambda = 5870$ Å and shifted by arbitrary constants for comparison purposes.

Including the integrated spectrum of Ruprecht 83, the present spectrum list increases to 47 integrated spectra and becomes, as far as we are aware, the largest available sample of integrated spectra of Galactic open clusters.

3 CONSTRUCTION OF TEMPLATES

The general rule for building the template spectra consists in making spectrum groups of clusters with ages within a limited age range. All the spectra were corrected for interstellar reddening using the values listed in Table 1. Moreover, they satisfy the requirement

[1] IRAF is distributed by the National Optical Astronomy Observatories, which is operated by the Association of Universities for Research in Astronomy, Inc., under contract with the National Science Foundation.

of having, within the respective age group, comparable continuum energy distributions and spectral absorption features. A total of 10 spectral groups representing cluster stages of 2–4, 5–10, 20, 40, 45–75, 100–150, 200–350, 500, 1×10^3, $3–4 \times 10^3$ Myr, respectively, finally resulted from the age distribution of the cluster sample. The age ranges of the resulting groups reflect the age dispersion of the involved spectra, without any remarkable difference being observed between spectra within the groups. Some age ranges also appear to show the existence of relatively short periods in the cluster spectral evolution, in which the integrated light becomes dominated by brighter stars with particular spectral signatures.

The template spectrum representative of an age group was built by averaging the integrated spectra in such a group, weighted by their squared S/N ratios. The S/N ratios were measured in regions virtually free from absorption and emission features common to all the spectra of the age group. Clusters affected by high interstellar reddening values have distinct S/N ratios in different parts of their spectra, the lower values being measured towards bluer wavelengths. For these cluster groups we decided to split up the spectra into two segments, the so-called 'blue' and 'red' spectra, assigning different weights to both parts according to the measured S/N ratios. Therefore, we accomplished a more appropriate use of the spectra by enhancing the best-defined regions and weakening the noisier parts of the spectra. The spectral groups have an average of four to five cluster spectra, with a minimum of two spectra. Only the template spectrum of the 500-Myr age group comes from the average of two high-quality integrated spectra (Ruprecht 115 and Lynga 11). Fig. 2 illustrates an example of the construction of the template spectra, where the template spectrum and the individual cluster spectra of the 200–350 Myr age group are shown normalized at $\lambda = 5870$ Å and shifted by arbitrary constants for comparison purposes.

We applied additional criteria to clusters younger than 30 Myr with emission features of nebular or circumstellar origin to build the corresponding templates. Nebular lines in the range 5–30 Myr

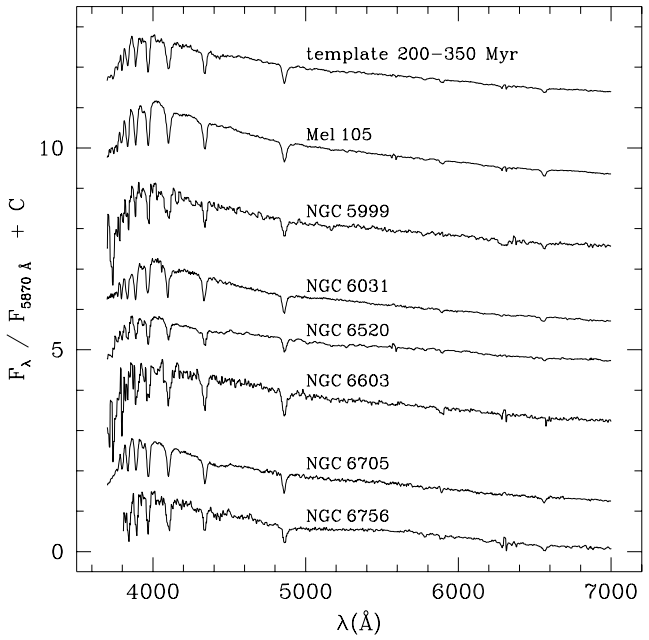

Figure 2. Integrated template spectrum for the 200–350 Myr age group and the individual cluster spectra of the group. The spectra are normalized at $\lambda = 5870$ Å and shifted by arbitrary constants for comparison purposes.

can occur in the integrated cluster spectra, as observed by Santos et al. (1995) in the Magellanic Clouds clusters. They are related to winds and supernova remnants, residual emission related to fossil H II regions, or diffuse emission in H II/OB associations, or even projection effects. Stars with extended atmospheres such as Be stars also occur in a similar age range (Mermilliod 1981a,b) and they show up in the integrated spectra of Magellanic Cloud clusters (Bica, Alloin & Santos 1990). Particularly for the 20-Myr age group, we did not take into account the spectral regions around Hα and the nebular lines [O II]$_{\lambda 3727}$, [N II]$_{\lambda 6584}$ and [S II]$_{\lambda\lambda 6717,6730}$ in the integrated spectrum of Ruprecht 119, since they correspond to the optical H II region G322.5–1.9 (Georgelin & Georgelin 1970), probably superimposed to or within the same complex as the cluster. These features do not appear in any of the other spectra of the group (Hogg 15, BH 217, NGC 6318, BH 245), justifying our procedure.

For the two youngest groups, namely the 2–4 and 5–10 Myr age groups, we carried out different spectrum combinations since the cluster spectra show evidence of a wide variety of scenarios, such as the presence of dominant luminous stars (supergiant stars), circumstellar emission (Wolf–Rayet and Be stars), nebular emission (clusters embedded in H II regions), and also spectra affected by internal reddening values caused by interstellar material distributed within the cluster boundaries. Two main templates were constructed for each age group to represent the synthesis of the integrated light of clusters having, on the one hand, only main-sequence (MS) stars and, on the other hand, other types of stars in addition to MS stars, such as Wolf–Rayet (WR), Be or supergiant (SG) stars. Each of these templates was corrected by interstellar reddening, taking into account the adopted $E(B-V)$ colour excess for individual clusters, which are mean values obtained primarily from colour–magnitude diagram (CMD) analyses (column 4 of Table 1), and foreground-reddening estimates provided by integrated spectrum studies (references in column 3 of Table 1), respectively. Note that foreground-reddening-corrected templates can be very useful in integrated spectroscopy studies of young clusters in the spiral arms of galaxies, where their continua are affected by the reddening produced in front of the clusters. When internal dust associated with the cluster exists, the spectroscopic reddening proves to be lower than the photometric one since the less reddened stars of a given spectral type should contribute to the integrated light with larger fluxes in comparison with the most reddened stars of the same spectral type. We calculated the individual cluster internal reddening values in the 2–4 and 5–10 Myr age groups from the difference between the photometric and spectroscopic $E(B-V)$ colour excesses, and derived averaged internal reddening values of 0.30 ± 0.10 and 0.15 ± 0.10, respectively. Thus, for each stellar combination we generated three distinct templates depending on whether the cluster spectra were reddening corrected by: (i) individual adopted $E(B-V)$ colour excesses; (ii) individual foreground $E(B-V)$ values; or (iii) foreground-reddening values computed from the difference between the adopted $E(B-V)$ values and the averaged internal values for the group. In summary, we produce a total of 12 templates for the 2–4 and 5–10 Myr age groups: two stellar combinations (MS stars and MS + other types of stars) per group, each one with three possible variants according to the reddening correction procedure employed (Figs 3 and 4).

4 SPECTRAL GROUPS

Table 2 lists the resulting template spectra and the member clusters associated to the different age groups. The first letter of the template indicates whether it corresponds to a young age group (Y) or

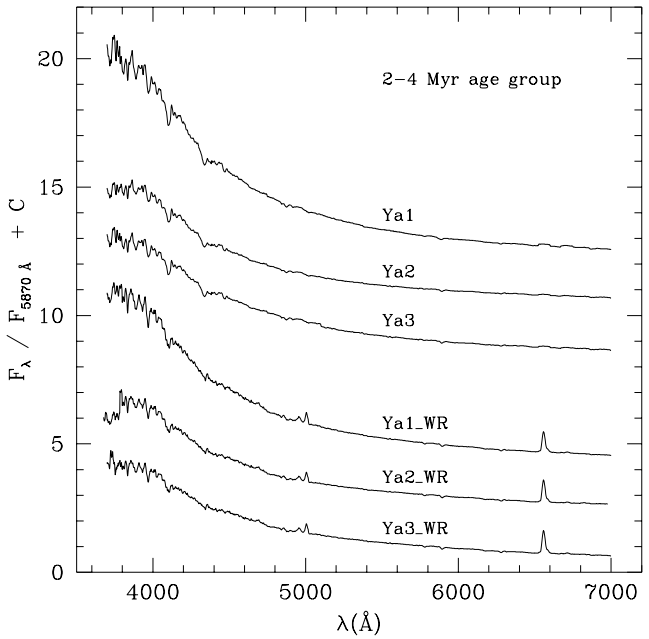

Figure 3. Galactic open-cluster template spectra for the 2–4 Myr age group. The spectra are normalized at $\lambda = 5870$ Å and shifted by arbitrary constants for comparison purposes.

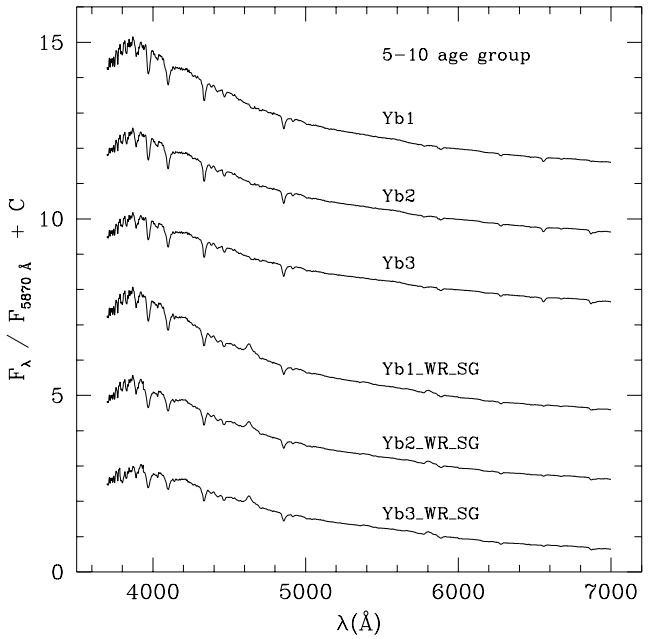

Figure 4. Galactic open-cluster template spectra for the 5–10 Myr age group. The spectra are normalized at $\lambda = 5870$ Å and shifted by arbitrary constants for comparison purposes.

to an intermediate-age group (I). Within young and intermediate-age groups, we used a second alphabetic character to identify different spectra, and included a third numeric character in the 2–4 and 5–10 Myr templates to differentiate cluster spectra corrected by: (i) mean cluster reddening; (ii) individual foreground reddening; or (iii) foreground reddening calculated taking into account an averaged internal reddening (see Section 3). Template spectra that contain WR and/or SG features are also clearly labelled. The resulting template spectra are shown in Figs 3–6, wherein they are normalized at $\lambda = 5870$ Å and shifted by arbitrary constants for the sake of comparison.

Table 2. Galactic open-cluster template spectra for different age groups.

Name	Age range (Myr)	Group members
Ya1	2–4	NGC 3293, Pismis 17, NGC 6611
Ya2		" "
Ya3		" "
Ya1_WR		Westerlund 2, NGC 3293, Pismis 17, NGC 3603, NGC 6611
Ya2_WR		" "
Ya3_WR		" "
Yb1	5–10	vdB-RN 80, Hogg 11, NGC 5606
Yb2		" "
Yb3		" "
Yb1_WR_SG		vdB-RN 80, Hogg 11, NGC 4755, NGC 5606, Westerlund 1, NGC 6231
Yb2_WR_SG		" "
Yb3_WR_SG		" "
Yc	20	Hogg 15, Ruprecht 119, BH 217, NGC 6318, BH 245
Yd	40	Pismis 22, NGC 6178, NGC 6216
Ye	45–75	NGC 2368, Ruprecht 83, Hogg 3, Bochum 12, Ruprecht 130
Yf	100–150	Haffner 7, ESO 429-SC 13, BH 87, BH 132, Ruprecht 120, Ruprecht 144
Yg	200–350	Melotte 105, NGC 5999, NGC 6031, NGC 6520, NGC 6603, NGC 6705, NGC 6756
Yh	500	Ruprecht 115, Lyngå 11
Ia	1×10^3	NGC 2635, NGC 2660, UKS 2, Pismis 18
Ib	$3–4 \times 10^3$	NGC 2158, Berkeley 75, ESO 93-SC 8, NGC 6253

Fig. 3 shows that, in addition to the contribution of luminous WR stars, the internal reddening in very young clusters (age $\sim$ 2–4 Myr) plays an important role in the resulting slope of the continuum energy distribution. The presence of WRs in the spectral synthesis of these very young clusters is recognized from their characteristic emission lines (Santos & Bica 1993). The internal reddening effect appears to be less significant in clusters with 5–10 Myr (see Fig. 4). In this age range, however, the sources that produce perceivable changes in the template spectral features are WR and/or SG stars. Likewise, we should remember that very young clusters can evolve from a pure H II region phase to another stage with massive stars eroding and blowing out the residual material from the star formation process, and, consequently, different amounts of dust from those causing an averaged internal extinction of $E(B-V)_{\rm internal} \sim$ 0.15–0.30 can be found within clusters. NGC 3293 behaves as a such transitional case. The cluster, embedded in the Gum 30 H II region in the Carina complex, is 6 ± 1 Myr old (see Table 1) and has stars of $\sim$3 Myr in the gravitational contraction phase (Baume 2001). Towards blue wavelengths, its integrated spectrum proves to be steeper than those of clusters in the 5–10 Myr age group and does not have Balmer lines as intense as in these latter spectra either. For this reason, we decided to include it in the slightly younger 2–4 Myr age group.

Figs 3–6 represent the spectral evolution up to intermediate ages of stellar populations around the Solar metallicity, which can be very useful, for example, for the analysis of stellar populations in

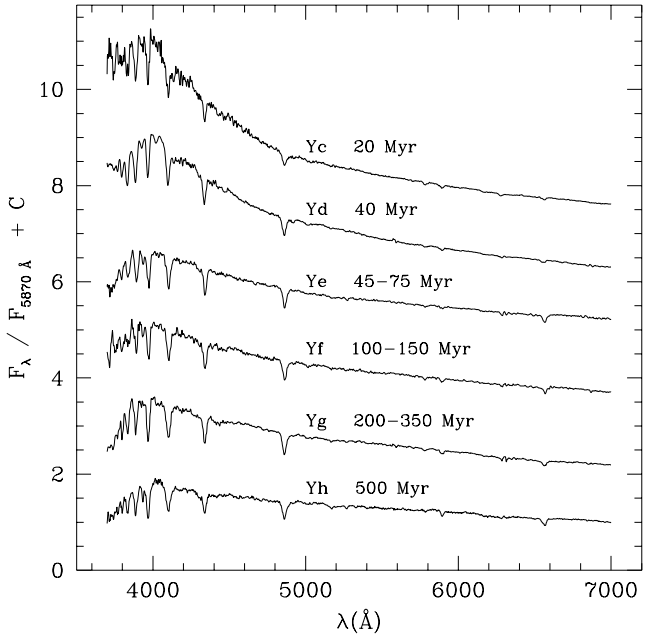

Figure 5. Galactic open-cluster template spectra for the 20, 40, 45–75, 100–150, 200–350 and 500-Myr age groups. The spectra are normalized at $\lambda = 5870$ Å and shifted by arbitrary constants for comparison purposes.

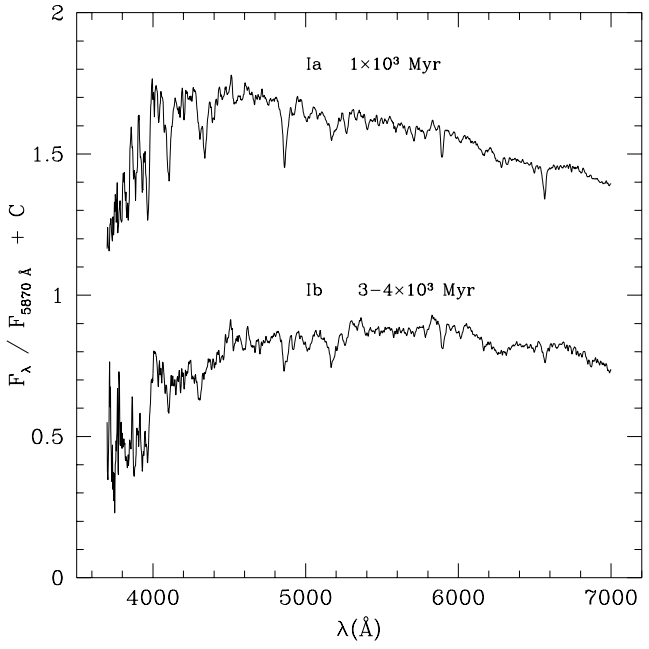

Figure 6. Galactic open-cluster template spectra for the 1×10^3, and 3–4 $\times 10^3$ Myr age groups. The spectra are normalized at $\lambda = 5870$ Å and shifted by arbitrary constants for comparison purposes.

discs of spiral galaxies and starbursts involving massive galaxies. In the 2–4 Myr template (Fig. 3) the MS-dominated spectrum should occur more often in less massive clusters owing to stochastic effects, while the larger population of stars in massive clusters makes the occurrence of WR stars more probable. The emission features in this template are mostly from WN stars. Less massive clusters in the 5–10 Myr stage will also be preferentially MS-dominated integrated spectra, while more massive clusters will more probably contain massive star evolution products such as WC stars and supergiants (Fig. 4). The strong emission feature at $\lambda = 4620$ Å is from a WC star in NGC 6231 (Santos & Bica 1993). The spectral evolution in the range 20–350 Myr is characterized by the change of continuum slope as the turn-off becomes fainter, accompanied by an increase of the Balmer jump and Balmer lines (Fig. 5). Metal lines such as K CaII, *G* band and Mg I become increasingly important at intermediate ages, especially at about 3–4 Gyr (Fig. 6). Between 500 Myr and 1 Gyr the flux below 4000 Å becomes dominated by the 4000-Å break instead of the Balmer jump, revealing the onset of the important contribution of giant branches to the integrated light.

4.1 Revised fundamental parameters for some individual clusters

The increased time resolution of the present template sequence, the use only of Galactic open clusters and/or the fact that their S/N ratio was improved by a larger available sample of individual clusters with respect to Bica (1988) and Santos & Bica (1993), allowed us to redetermine the parameters of some particular clusters more confidently. We paid particular attention to clusters with reddening values and ages coming from the comparison of their integrated spectra with template spectra. By comparing the cluster integrated spectra with template spectra adjacent in age, we could improve the matching and re-estimate the cluster fundamental parameters.

NGC 2635. Ahumada et al. (2001) obtained from the cluster integrated spectrum a colour excess $E(B-V) = 0.05 \pm 0.03$ and an age $t = 1500 \pm 500$ Myr. They found that the I1 template (1 Gyr, Bica 1988) best matches the cluster spectrum and that the equivalent widths of the Balmer lines suggest an age of $t \approx 2$ Gyr. On the other hand, using CCD *UBVRI* photometry, Moitinho (2001a,b) recently estimated $E(B-V) = 0.35$, $m - M = 14.89$ and $t = 300$ Myr for the cluster. The cluster age was derived from the fit of theoretical isochrones computed by Bertelli et al. (1994) to the cluster CMD. The fitted isochrone properly matches the cluster MS, although it appears to be placed following the lower MS envelope and not the mean cluster star positions, but turns out to be notably redder than the observed giant clump. We counted a total of eight stars defining the giant clump of the cluster, which are $\Delta(V-I) \approx 0.65 \pm 0.10$ mag to the right of the cluster turn-off. The differences between the $V-I$ colours of the MS turn-off and the giant clump predicted by Bertelli et al. (1994) for isochrones of 300 and 1×10^3 Myr are 0.95 and 0.65, respectively, which suggests that the cluster should be older than ~800 Myr. Additionally, since the giant clump is at the same magnitude level as the turn-off, the cluster should not be older than 1.5×10^3 Myr (Phelps, Janes & Montgomery 1994). Likewise, its integrated spectrum compares well with the integrated spectra of clusters in the 1×10^3 Myr age group, when corrected by $E(B-V) = 0.25 \pm 0.05$, which is also clearly suggested by the equivalent width of the Hδ line. Although more detailed studies are necessary to state the cluster fundamental parameters more precisely, we suggest the present values of age and reddening for NGC 2635 (see Table 1).

Hogg 12. The object was considered by Moffat & Vogt (1975) as a random fluctuation of the field star density. They observed photoelectrically 11 stars in the *UBV* system, nine of them being distributed along a vertical MS in the (V, $B-V$) CMD, similar to stars of a poorly populated young open cluster. Ahumada et al. (2001) obtained integrated spectra for this group and determined a mean age of $t = 85 \pm 15$ and $E(B-V) = 0.04$ by template

matching. Using their $E(B-V)$ value, we found that the Ye template matches the cluster spectrum appropriately. This result is compatible with the idea of the existence of a young open cluster, as judged from the distribution of the stars observed by Moffat & Vogt (1975) in the CMD. On the other hand, the Ca II K line (3933 Å), a feature commonly seen in F-type MS stars, appears weaker in the spectrum of Hogg 12 than in the Ye template, which is an indication that the object could have lost its lower MS. On the basis of this assumption, the integrated spectrum would be showing the upper MS of a cluster, equivalent to that of a populous cluster of the same age, since the massive (brighter) stars dominate the integrated flux. Such an object could be catalogued as a dissolving star cluster candidate (Bica et al. 2001; Pavani et al. 2001) with the disintegration phenomenon occurring at a young age. Note that cluster disintegration depends on the cluster initial mass and position in the Galaxy. Although we favour the cluster reality of Hogg 12, we decided not to include it in the template cluster sample.

BH 217. This is a clear example of improvement of the estimated cluster fundamental properties owing to a more complete sample of template spectra. Ahumada et al. (2000) previously determined $E(B-V)=0.80\pm0.03$ and $t=35\pm15$ Myr. Their adopted age comes from the average between the age measured using the equivalent widths of the Balmer lines, which is independent of the reddening effect, and the age of the Y2 template (50 Myr, Bica 1988), which most resembles the cluster spectrum. However, the cluster spectrum does not match the present Yd and Ye templates, if it is corrected by $E(B-V)=0.8$. A satisfactory solution is achieved when comparing its integrated spectrum, corrected by $E(B-V)=1.4\pm0.1$, with cluster spectra in the 20-Myr age group. This result is in excellent agreement with the previous derived Balmer age. Thus, we adopt for the cluster the present $E(B-V)$ colour excess and an age of 20 ± 15 Myr.

5 CONCLUDING REMARKS

We study the integrated spectral evolution in the range $3600<\lambda<7400$ Å of 47 Galactic open clusters, from those associated with gas emission until ages as old as a few Gyr. 20 new high S/N templates representing cluster evolutionary stages of 2–4, 5–10, 20–40, 45–75, 100–150, 20–350, 500, 1×10^3 and 3–4 $\times10^3$ Myr are presented. These new templates as well as the CASLEO and LNA collection of 39 open-cluster spectra are made available as a library at CDS. Additionally, we present the flux-calibrated integrated spectrum of the loose open-cluster Ruprecht 83, also known as BH 80. Using the equivalent widths of the Balmer lines and comparing the cluster spectrum with cluster spectra of known parameters, we derive $E(B-V)=0.40\pm0.15$ and an age of 55 ± 20 Myr for Ruprecht 83. Using the present template library we revised the fundamental parameters of the small angular size open clusters NGC 2635, Hogg 12 and BH 217. The latter is a clear example of how a more complete sample of template spectra allows for improvement of the estimated cluster fundamental parameters. The present template sequence represents the solar metallicity spectral evolution of a single-aged stellar population, with potential applications to population synthesis and the interpretation of composite stellar populations in star-forming giant galaxies.

ACKNOWLEDGMENTS

We thank the CASLEO staff for their hospitality and assistance during the observations. We also acknowledge use of the CCD and data acquisition system supported under US National Science Foundation grant AST-90-15827 to R. M. Rich. This work was partially supported by the Brazilian institutions CNPq and FINEP, and the Argentinian institutions CONICET, SECYT (Universidad Nacional de Córdoba), AGENCIA CóRDOBA CIENCIA and AGENCIA NACIONAL DE PROMOCIóN CIENTFICA Y TECNOLóGICA (ANPCyT). Thanks are also due to A. Moitinho who kindly sent us the CMDs and the derived fundamental parameters of NGC 2635. Based on observations made at Complejo Astronómico El Leoncito, which is operated under agreement between the Consejo Nacional de Investigaciones Cientficas y Técnicas de la República Argentina and the National Universities of La Plata, Córdoba and San Juan, Argentina.

REFERENCES

Ahumada A. V., Clariá J. J., Bica E., Piatti A. E., 2000, A&AS, 141, 79
Ahumada A. V., Clariá J. J., Bica E., Dutra C., Torres M. C., 2001, A&A, 377, 845
Balona L. A., 1994, MNRAS, 267, 1060
Baume G., 2001, PhD. thesis, Univ. of La Plata, Argentina
Baume G., Vázquez R. A., Feinstein A., 1999, A&AS, 137, 233
Belikov A. N., Kharchenko N. V., Piskunov A. E., Schilbach E., 1999, A&AS, 134, 525
Belikov A. N., Kharchenko N. V., Piskunov A. E., Schilbach E., 2000, A&A, 358, 886
Bertelli G., Bressan A., Chiosi C., Fagotto F., Nasi E., 1994, A&AS, 106, 275
Bica E., 1988, A&A, 195, 76
Bica E., Alloin D., 1986a, A&A, 162, 21
Bica E., Alloin D., 1986b, A&AS, 66, 171
Bica E., Alloin D., 1987, A&A, 186, 49
Bica E., Alloin D., Santos J. F. C. Jr, 1990, A&A, 235, 103
Bica E., Ortolani S., Barbuy B., 1993, A&A, 270, 117
Bica E., Clariá J. J., Piatti A. E., Bonatto C., 1998, A&AS, 131, 483
Bica E., Ortolani S., Barbuy B., 1999, A&AS, 136, 363
Bica E., Ortolani S., Barbuy B., 2000, A&AS, 145, 399
Bica E., Santiago B. X., Dutra C. M., Dottori H., de Oliveira M. R., Pavani D. B., 2001, A&A, 366, 827
Bragaglia A., Tessicini G., Tosi M., Marconi G., Munari U., 1997, MNRAS, 284, 477
Brocato E., Castellani V., Digiorgio A., 1993, AJ, 105, 2192
Christian C. A., Heasley J. N., Janes K. A., 1985, ApJ, 299, 683
Delgado A. J., Alfaro E. J., Cabrera-Caño J., 1997, AJ, 113, 713
Feinstein A., Marraco H. G., 1980, PASP, 92, 266
Georgelin Y. P., Georgelin Y. M., 1970, A&A, 6, 349
Gutiérrez-Moreno A., Moreno H., Cortés G., Wenderoth E., 1988, PASP, 100, 973
Hartwick F. D. A., Hesser J. E., 1973, ApJ, 183, 883
Herbst W., Miller D. P., 1982, AJ, 87, 1478
Hillenbrand L. A., Massey P., Strom S. E., Merrill K. M., 1993, AJ, 106, 1906
Hofmann K. H., Seggewiss W., Weigelt G., 1995, A&A, 300, 403
Jablonka P., Alloin D., Bica E., 1992, A&A, 260, 97
Jablonka P., Bica E., Pelat D., Alloin D., 1996, A&A, 307, 390
Jablonka P., Bica E., Bonatto C., Bridges T. J., Langlois M., Carter D., 1998, A&A, 335, 867
Johnson H. L., Sandage A. R., Wahlquist H. D., 1956, ApJ, 124, 81
Kjeldsen H., Frandsen S., 1991, A&AS, 87, 119
Melnick J., Tapia M., Terlevich R., 1989, A&A, 213, 89
Mermilliod J.-C., 1981a, A&A, 97, 235
Mermilliod J.-C., 1981b, A&AS, 44, 467
Moffat A. F. J., Vogt N., 1973, A&AS, 10, 135
Moffat A. F. J., Vogt N., 1975, A&AS, 20, 125
Moitinho A., 2001a, A&A, 370, 436
Moitinho A., 2001b, PhD. thesis, UNAM, Mexico

Pandey A. K., Ogura K., Sekiguchi K., 2000, PASJ, 52, 847
Pavani D. B., Bica E., Dutra C. M., Dottori H., Santiago B. X., Carranza G., Diaz R. J., 2001, A&A, 374, 554
Phelps R. L., Janes K. A., Montgomery K. A., 1994, AJ, 107, 1079
Piatti A. E., Clariá J. J., 2001, A&A, 370, 931
Piatti A. E., Bica E., Clariá J. J., 1998a, A&AS, 127, 423
Piatti A. E., Clariá J. J., Bica E., Geisler D., Minniti D., 1998b, AJ, 116, 801
Piatti A. E., Clariá J. J., Bica E., 1999, MNRAS, 303, 65
Piatti A. E., Bica J. J., Clariá J. J., 2000a, A&A, 362, 959
Piatti A. E., Clariá J. J., Bica E., 2000b, A&A, 360, 529
Piatti A. E., Bica E., Santos J. F. C. Jr, Clariá J. J., 2002, A&A, 387, 108
Sagar R., Cannon R. D., 1995, A&AS, 111, 75
Sagar R., Griffiths W. K., 1998, MNRAS, 299, 1
Sandrelli S., Bragaglia A., Tosi M., Marconi G., 1999, MNRAS, 309, 739
Sanner J., Brunzendorf J., Will J. M., Geffert M., 2001, A&A, 369, 511
Santos J. F. C. Jr, Bica E., 1993, MNRAS, 260, 915
Santos J. F. C. Jr, Bica E., Clariá J. J., Piatti A. E., Girardi L. A., Dottori H., 1995, MNRAS, 276, 1155
Santos J. F. C. Jr, Alloin D., Bica E., Bonatto C., 2001, in Proc. IAU Symp. 207, in press
Stone R. P. S., Baldwin J. A., 1983, MNRAS, 204, 347
Sung H., Bessell M. S., Lee S. W., 1998, AJ, 115, 734
Sung H., Bessell M. S., Lee H. W., Kang Y. H., Lee S. W., 1999, MNRAS, 310, 982
Topaktas L., Fenkart R. P., 1982, A&AS, 49, 475
Turner D. G., Grieve G. R., Herbst W., Harris W. E., 1980, AJ, 85, 1193
van den Bergh S., Hagen G. L., 1975, AJ, 80, 11
Vázquez R. A., Baume G., Feinstein A., Prado P., 1994, A&AS, 106, 339

APPENDIX A: NEAR-IR INTEGRATED SPECTRA

During our previous studies with CASLEO data we obtained spectra covering the near-IR range (≈7000–9200 Å). In young clusters several features of interest can occur such as TiO bands, Ca II triplet and Paschen lines (Bica & Alloin 1987). We dispose of near-IR spectra for 21 clusters (UKS 2, Westerlund 2, ESO 93-SC8, Melotte 105, BH 132, Pismis 18, NGC 6031, Ruprecht 115, Pismis 22, Ruprecht 119, Ruprecht 120, NGC 6178, Lyngå 11, Westerlund 1, NGC 6216, NGC 6253, BH 217, NGC 6318, BH 245, Ruprecht 130 and Ruprecht 144). The paper sources are the same ones as indicated in column 3 of Table 1. They were not numerous enough to create templates with a suitable time resolution, but we will include them in the CDS library in view of future template developments in the near-IR range.

This paper has been typeset from a TEX/LATEX file prepared by the author.